International Journal for Research in Engineering Application & Management (IJREAM)
ISSN : 2454-9150 Vol-08, Issue-04, July 2022

Fuzzy Logic Control Based Bidirectional DC/DC/AC Converter for Grid and Electric Vehicle Hybrid Energy Storage System

Dr. J. Srinu Naick, Professor, EEE Department, Chadalawada Ramanamma Engineering College, Tirupati, Andhra Pradesh, India, speaksrinu@gmail.com.

P.Theertha, B.Tech. Student, EEE Department, Chadalawada Ramanamma Engineering College Tirupati, Chittoor, Andhra Pradesh, India.

Abstract— As EVs gain popularity, charging technologies must improve. Power conversion and control are needed for renewable energies, distributed generation, energy storage, and electric cars. In hybrid systems, this approach is generally performed in two steps, increasing power losses and expenses. Inverters, fuel cells, hybrid and electric vehicles, and ac/dc microgrids use this setup. Most three-port topologies include numerous power processing steps for connected elements. As EVs gain popularity, demand for grid electricity to recharge them will rise. V2G links electric vehicles with the grid to satisfy demand and reduce recharging impact. V2wide G's data network serves the grid, charging stations, and electric automobiles. Erroneous V2G data may exist. Unfixed faults will destabilize the grid. V2G controller allows electric car grid integration. This research presented a two-layer intelligent controller with data integrity and rectification check blocks and a fuzzy logic controller (FLC). The recommended controller is tested using a simulation model with an electrical and communication network. The results show how an intelligent controller can decrease mistake impact by balancing grid-to-EV power. The intelligent controller's potential is shown by comparison to the ordinary FLC.

Index Terms—Three-port converters, bidirectional ac-dc converters, battery energy storage systems, multi-port converters, model predictive control.

I. INTRODUCTION

Hybrid dc/ac power systems are becoming more prevalent due to solar PV, battery energy storage systems (BESS), fuel cells, datacenters, and ac/dc microgrids. Renewable energy sources and highly nonlinear demands, such as EV charging stations, have modified how the traditional ac-grid interacts with dc elements [1]–[3]. Two or more power converters must govern the interplay between ac motors and dc sources in EV power trains [4]. Power converters that manage bidirectional power flow between ac and dc loads and sources are prevalent [1], [5].

Hybrid EV power trains or grid-connected PV-BESS systems stand out among hybrid designs with two dc ports tied to an ac system [6]–[9]. PV micro-inverters need a boost stage. PV transformer less string inverters need a minimum number of PV modules to eliminate the boost stage, while hybrid PV-BESS inverters need two power converters to integrate PV and BESS with the ac grid. Single - phase grid connected inverters produce a double frequency ripple in the dc-link, which can damage the battery or MPPT. Hybrid cars, like fuel cell electric vehicles, use dc-dc converters to connect the fuel cell and batteries to the inverter dc-link.

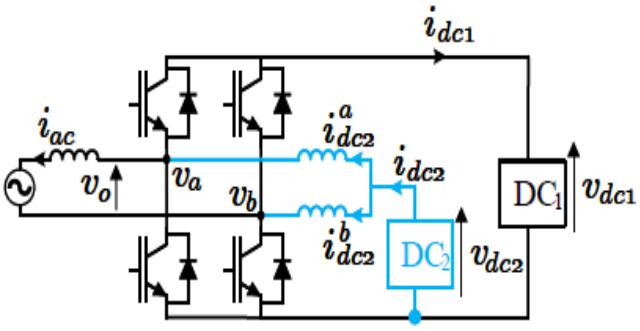

(a)

 DOI : 10.35291/2454-9150.2022.0387

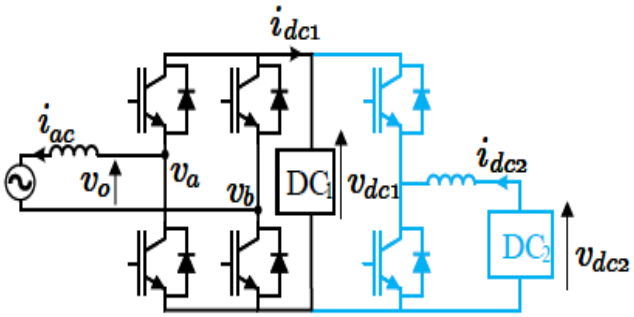

(b)

Fig.1.(a) Proposed single-phase TPC. (b) Conventional h-bridge and buck boost for dc/dc/ac system.

Three-port converters (TPC) offer increased power density, fewer components, and improved efficiency [10]. TPC topologies focus on soft-switched converters or modified PWM.

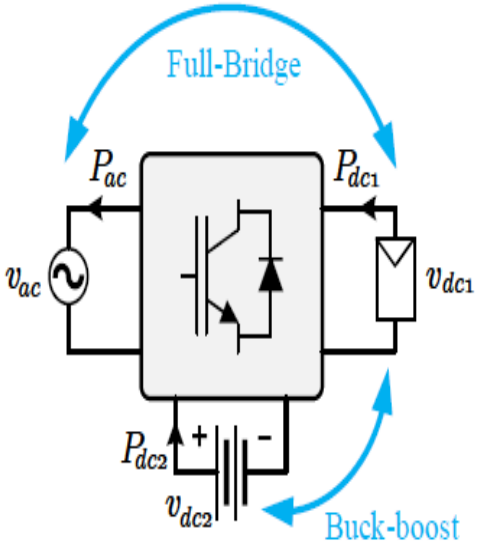

Fig. 2. Proposed TPC for a PV-BESS application.

In soft-switched solutions, the first stage contains three dc ports and the second stage incorporates a dc/ac converter [9], [11],–[13]. The second step to link the ac system affects the first stage's (dc/dc conversion) efficiency. Modified PWM TPC systems use active and passive components and offer superior control and modulation techniques [14]–[18]. The second TPC technique reduces power losses, component count, and failure rate. This study proposes a bidirectional TPC to connect two dc ports with single-phase or three-phase ac. Each converter port can link power sources or loads. Each inverter leg is a buck-boost converter, simplifying the architecture. Fig. 1 shows how this buck-boost converter employs the same number of semiconductors as typical inverters and adds one inductor per leg. FCS-MPC regulates power flow across ports using MIMO state-space modeling. Simulations and experiments show the recommended converter's bidirectional performance and boost ability, allowing low dc voltage to be linked to the ac grid without a transformer. The proposed approach only comprises one power conversion stage between dc and ac ports, unlike earlier three-port converters. Previous TPC topologies required more stages or high-power transistors to do the same tasks. The suggested solution improves power density and flexibility because all ports are bidirectional. This is possible thanks to a proposed control technique that governs power transfer between the three ports by performing a coupled computation of two controlled variables (va; vb).

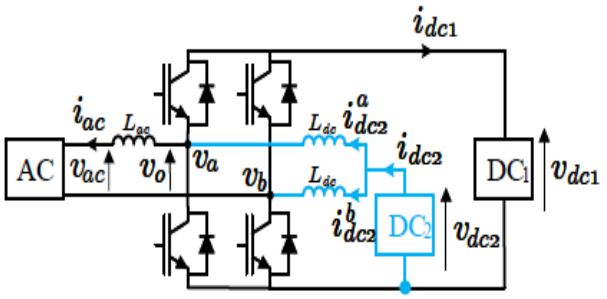

Fig. 3. (a) Proposed single-phase TPC

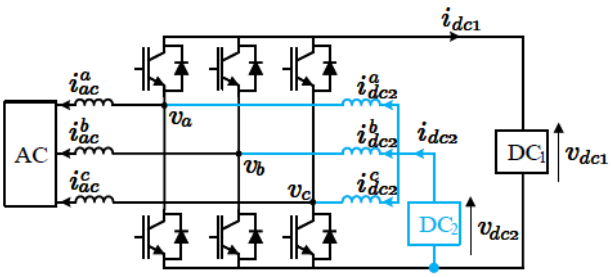

(b)

Fig. 3. (b) Proposed three-phase TPC

II. Existing Method of Three Port Converter (TPC)

The Existing method of TPC is based on a full-bridge converter with each leg acting as a buck-boost converter at the same time. As a result, the ac port and the dc1 port interact similarly to a normal full-bridge, whereas the dc2 port and the dc1 port interact similarly to a conventional buck-boost converter (see Fig. 2). The architecture is straightforward, but the simultaneous operation as a full-bridge and buckboost converter necessitates multi-variable control in order to accomplish three-port governance. As demonstrated in Fig. 3, the TPC can be used in single-phase or three-phase designs. The dc2 port is decoupled from the ac side and can operate at a lower voltage than the dc1 port, which has a minimum value set by the peak ac voltage. PV modules, batteries, capacitors, fuel cells, and dc micro-grids are examples of different sorts of sources or loads that could be represented by both dc ports. The ac systems could represent the grid, an ac motor or load, or an ac generator, among other things. The type of sources/loads, on the other hand, will set constraints and

 DOI : 10.35291/2454-9150.2022.0387

specific control goals for the system's voltages and currents[4].

A. Operation Principle:

A new degree of freedom is required in order to controlthe power at the new third port, as conventional linear control schemes just regulate one variable between two ports. Thus, instead of using only vo as manipulated variable, the required controller should regulate both va and vb separately to control the currents at all ports.

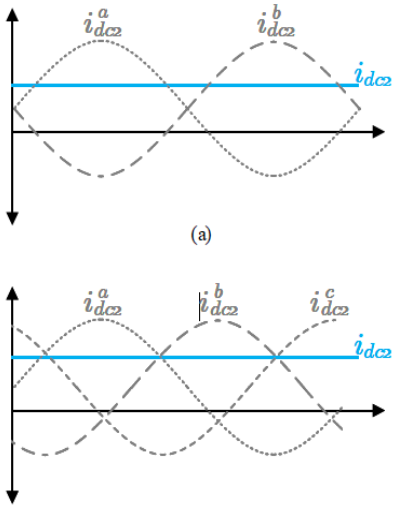

Fig. 4. Current waveforms of the second dc port inductors. (a) Single-phase TPC. (b) Three-phase TPC.

The change from one to two manipulated variables provides the capability to control iac and idc2 at the same time. The dynamical equations (1)-(2) describe the behaviour of the regulated variables for the single-phase case.

$$\frac{di_{ac}}{dt} = \frac{1}{L_{ac}}(\overbrace{(v_a - v_b)}^{v_o} - r_{ac} \cdot i_{ac} - v_{ac}) \quad (1)$$

$$\frac{di_{dc2}}{dt} = \frac{1}{L_{dc}}(2v_{dc2} - (v_a + v_b) - r_{dc} \cdot i_{dc2}) \quad (2)$$

The current idc2 is generated by the sum of the currents of the interface inductors Ldc. These currents contain both dc and ac components defined by the voltage vdc2 and the voltages va and vb from the converter legs. The oscillating component at the frequency of the ac port is canceled at the dc2 port by using 180_ phase-shift between the inductor currents, as it is shown in Fig. 4(a).

B. Voltage and Power Characteristics

The design of the converter (component sizing and control scheme) depends on the systems to be connected at each port, as they could require voltage or current control and unidirectional or bidirectional power flow[6]. Therefore, in order to characterize the topology, with a capacitor at dc1, a battery at dc2 and the single-phase grid at the ac side. This configuration allows to: connect a battery to the grid with a small capacitance at the dc-bus, as the battery is placed at the second dc-port which is free of low-frequency harmonics; and reduce the required series connected battery cells, as vdc2 can be lower than the peak voltage at the ac port. Furthermore, an additional source as a PV can be connected in parallel with the capacitor at dc1 to use the converter in a hybrid PV-BESS application. Thus, the following analysis applies to grid-connected BESS with boost capability and hybrid PV-BESS also connected to the ac-grid.

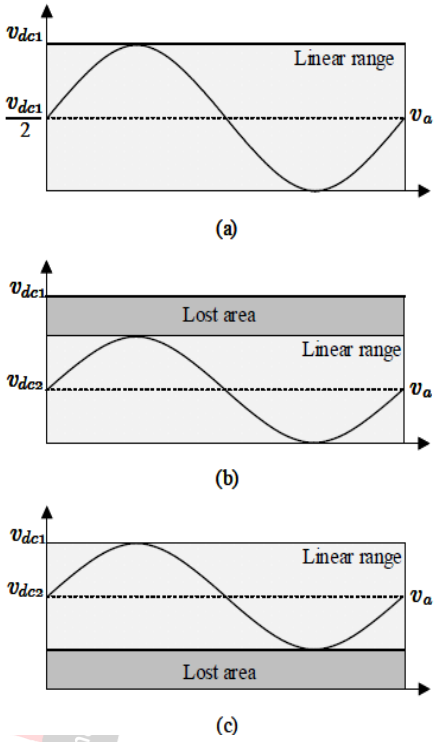

Fig. 5. Operating range for leg voltages. (a) Regular h-bridge. (b) Proposed TPC with vdc2 < 0:5 _ vdc1. (c) Proposed TPC with vdc2 > 0:5 _ vdc1

In the proposed TPC, voltage ratio between vdc2 and vdc1 defines the dc component of the voltages va and vb generated by the legs of the converter. This bias is highly relevant as it determines the maximum peak voltage of vo. In a regular h-bridge, the dc component for each leg is always 0:5vdc1, thus each voltage could use the entire linear range to generate the sinusoidal component. However, in the TPC topology, variations on the vdc2 voltage reduce the useful linear range and hence limit the maximum output voltage[11], as it is shown in Fig. 5. Consequently, in order to use the full voltage range at the ac output, the relation between both dc voltages should be vdc2 = 0:5vdc1. However, different voltage ratios and rated power can be selected according to the application. Considering the mentioned applications with a battery at dc2, the variations on the voltage depending on the state of charge should be included in the design to determine the limits of the operating range. The active power at the ac port is characterized by (3), where Vo and Vac represent

 DOI : 10.35291/2454-9150.2022.0387

the magnitudes of the output and grid voltages respectively and δ is the phase angle between both voltages. The power equation is the same of a regular dc/ac converter, but the exposed limitation on the output voltage should be considered according to (4). Therefore, the power characteristic depends on the relation of the dc voltages.

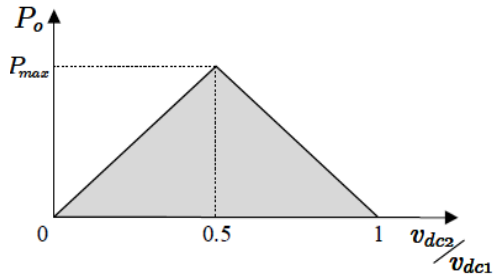

Fig. 6. Output power range vs. vdc2=vdc1 ratio

and it is shown in Fig. 6, where δ is determined by the power factor delivered.

$$P_o = \frac{V_o \cdot V_{ac}}{X_{Lac}} \sin(\delta) \quad (3)$$

$$V_o^{max} = \begin{cases} 2 \cdot v_{dc2} & v_{dc2} \le 0.5 \cdot v_{dc1} \\ 2 \cdot (v_{dc1} - v_{dc2}) & v_{dc2} > 0.5 \cdot v_{dc1} \end{cases} \quad (4)$$

III. CONTROL METHOD OF THE TPC

The proposed configuration in Fig. 3(a) presents three variables to be controlled (vo, idc2, vdc1) and two manipulated variables (va, vb). Thus, a multiple-input and multiple-output (MIMO) state-space approach was chosen to model and control the dynamics of the converter. Each manipulated voltage is determined by the switching state of the respective leg and the dc bus voltage as vi = Si . vdc1 with i ε $\{a, b\}$, s_1 ε $\{1,0\}$. Consequently, the proposed model (5) presents nonlinear terms given by the product of control inputs with state variables[7].

$$\underbrace{\frac{d}{dt}\begin{bmatrix} i_{ac} \\ i_{dc2} \\ v_{dc1} \end{bmatrix}}_{x} = \begin{bmatrix} \frac{1}{L_{ac}}(v_{dc1} \cdot (S_a - S_b) - r_{ac} \cdot i_{ac} - v_{ac}) \\ \frac{1}{L_{dc}}(2v_{dc2} - v_{dc1} \cdot (S_a + S_b) - r_{dc} \cdot i_{dc2}) \\ \frac{1}{C}(i_{ac} \cdot (S_b - S_a) + i_{dc2}^a \cdot S_a + i_{dc2}^b \cdot S_b) \end{bmatrix} \quad (5)$$

A Finite Control Set Model Predictive Control (FCS-MPC) was chosen to control the converter, given the multi-variable and non-linear characteristic of the system. In order to implement the controller, the model in (5) is converted to its discrete-time equivalent using the forward Euler approximation. Thus, the controller generates the switching states of each leg by performing an minimization of the cost function in (6) with the error of the three controlled variables.

$$\begin{aligned} J(k+1) = & \lambda_1 (i_{ac}(k+1) - i_{ac}^*)^2 + \\ & \lambda_2 (i_{dc2}(k+1) - i_{dc2}^*)^2 + \\ & \lambda_3 (v_{dc1}(k+1) - v_{dc1}^*)^2 \end{aligned} \quad (6)$$

The overall control scheme, shown in Fig. 7, includes an outer PI controller and a reference generator besides the FCS-MPC. The PI controller address the capacitor voltage variations due to the inherent losses of the components of the converter.

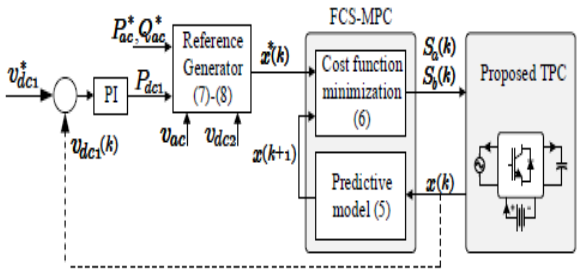

Fig. 7 Control Scheme of FCS-MPC for the proposed TPC.

The output of this outer controller is used, together with the power references at the ac side, to generate the current references for the grid and the battery ports following equations (7)-(8). Then, the MPC controller calculates the optimum signals Si to drive the converter according to the calculated references. The power balance that led to (8) considers that the power required to keep the voltage of the capacitor (Pdc1) will be addressed by the source delivering active power (either the grid or the battery).

$$i_{ac}^* = \frac{P_{ac}^*}{v_{ac} \cdot \cos(\phi)} \quad with \quad \phi = \arctan\left(\frac{Q_{ac}^*}{P_{ac}^*}\right) \quad (7)$$

$$i_{dc2}^* = \frac{P_{ac}^* + P_{dc1}}{v_{dc2}} \quad (8)$$

A fuzzy control system is based on fuzzy logic, a mathematical system that evaluates analogue input values in terms of continuous logical variables between 0 and 1. Classical or digital logic operates on discrete values of 1 or 0. (true or false, respectively). Machine control uses fuzzy logic. Fuzzy logic deals with things that cannot be represented as "true" or "false" rather as "partially true." Although evolutionary algorithms and neural networks can perform as well as fuzzy logic, fuzzy logic has the benefit that the answer can be expressed in terms that human operators can comprehend, so their experience can be incorporated in the design of the controller. This makes mechanising human-performed jobs easier. In a fuzzy control system, input variables are mapped by "fuzzy sets" of membership functions. "Fuzzification" converts a crisp input to a fuzzy value[16]. A control system may also incorporate switch, or "ON-OFF," inputs along with its analogue inputs. Such switch inputs will always have a truth value of 1 or 0, but the scheme can treat them as

 DOI : 10.35291/2454-9150.2022.0387

simplified fuzzy functions. The microcontroller decides what action to perform based on "mappings" of input variables into membership functions and truth values. WHEN BRAKES ARE WARM AND SPEED IS SLOW, BRAKE PRESSURE IS LOWERED. "Brake temperature" and "speed" are fuzzy set input variables. "Brake pressure" is a fuzzy output variable that can be "static" or "slightly increased".

IV. FUZZY CONTROL

Fuzzy controls are straightforward. Input, processing, and output. The input stage maps sensors, switches, thumbwheels, etc. to membership functions and truth values. The processing stage invokes each rule, generates a result for each, and combines the results. The output stage translates the combined result into a control output. Most membership functions are triangular, but trapezoidal and bell curves are also employed. The shape is less significant than the quantity and positioning of curves[9][13].

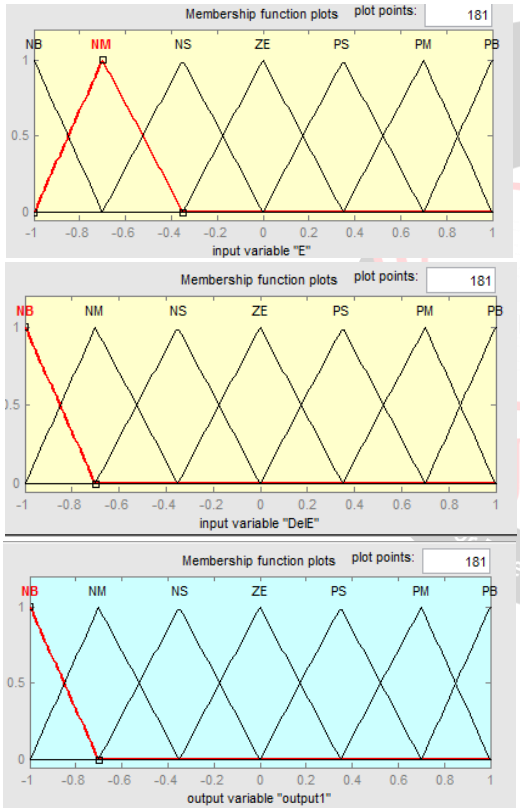

Fig 8 Example figures of input and output membership functions

Fuzzy control system design is based on empirical methods, basically A methodical approach to trial and-error . The general process is as follows:

- Document the system's operational specifications and inputs and outputs.
- Document the fuzzy sets for the inputs.
- Document the rule set.
- Determine the defuzzification method.
- Run through test suite to validate system, adjust details as required.
- Complete document and release to production.

This mechanism is divided into three parts. First, using input membership functions the inputs are fuzzified and then based on rule bases and inference system, outputs are produced and finally the fuzzy outputs are defuzzified and applied to the system. Error and the error change rate are selected as inputs. The block diagram of fuzzy control is represented as follows:

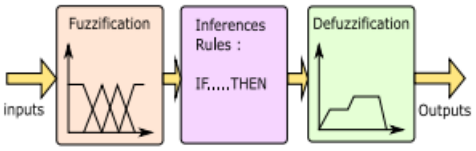

Generally, the design of a fuzzy controller for the control of electric drives requires the choice of the following parameters: linguistic variables, membership functions, inference method , and defuzzification strategy. Fuzzy controller inputs are the error and its derivative, while the output is the command itself. Triangular and trapezoidal membership functions are used on a universe of discourse normalized in the range [-1; 1] for each variable as shown in Fig.8 respectively for the inputs (error, error variation) and output (input process). The subsets fuzzy membership were noted as follows: BN: Big- Negative; SN: Small-Negative; AZ: About-Zero; SP: Small-Positive; BP: Big Positive. The fuzzy rules, for determining output variable of the controller as a function of input variables are grouped in the Table 1.

Table 1 :Inference matrix

Δu		e				
		BN	SN	AZ	SP	BP
Δe	BN	BN	BN	SN	SN	AZ
	SN	BN	SN	SN	AZ	SP
	AZ	BN	SN	AZ	SP	BP
	SP	BN	AZ	SP	SP	BP
	BP	AZ	SP	SP	BP	BP

Fig.9 shows the surface generated by the fuzzy system.

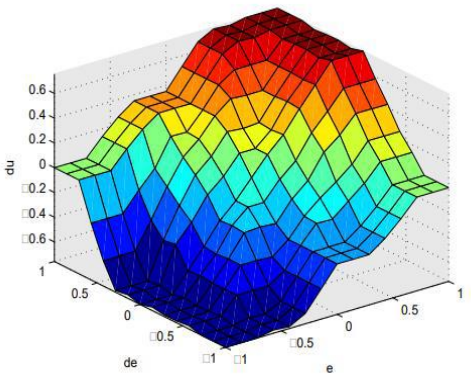

 DOI : 10.35291/2454-9150.2022.0387

Fig 10 Surface generated by the fuzzy system

The simulation results for the single-phase and three-phase TPCs in Figure 11 are presented in this section. Both configurations described in section II are considered in the single-phase case: a grid-connected BESS that takes advantage of the TPC's boost capabilities; and a hybrid PV-BESS system that provides consistent power to the grid while using the battery as an energy buffer. The three-phase instance, on the other hand, investigates a hybrid system with two dc sources and an ac load.

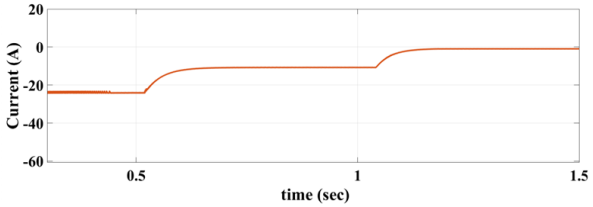

Fig. 11. Simulation results for the single-phase TPC used as a boost inverter for Battery current

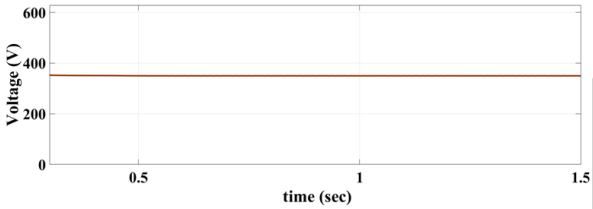

Fig. 12. Simulation results for the single-phase TPC used as a boost inverter for Capacitor voltage

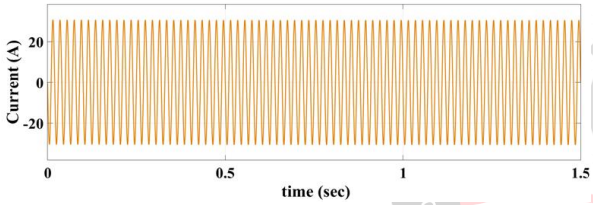

Fig. 13. Simulation results for the single-phase TPC used as a boost inverter for Grid current

In the defined power range, the converter performs correctly; Fig. 11 displays the response of the system's variables as the output power increases from 0.4 to 3 kW. The battery current in Fig. 11(a) is free of low-frequency harmonics and closely tracks the reference with only minor overshoots during step shifts. At the maximum power need, the dc bus voltage is kept at the desired value with a maximum ripple of 10% (Fig. 11(b)). As demonstrated in Fig. 11, the last port, which corresponds to the ac side, has a correct current response with fast tracking of the sinusoidal reference (c). Furthermore, when an active power source such as a PV is attached to the dc1 port, the previously proven regulation of the battery current can be used to supply a steady power output to the ac-grid. This is the second configuration for the single phase scenario, which uses port dc1 as a bidirectional energy buffer and port dc1 as a Unidirectional active power supply. The power response of the system to a change in PV generation[14] is shown in Fig. 12(a), where the battery delivers or absorbs power to address the three-port balance. Despite differences in the power given at dc1, the bidirectional performance of the battery port is shown in Fig. 12(b), where the regulated current changes correspondingly to keep the ac current constant (Fig. 12(c)).

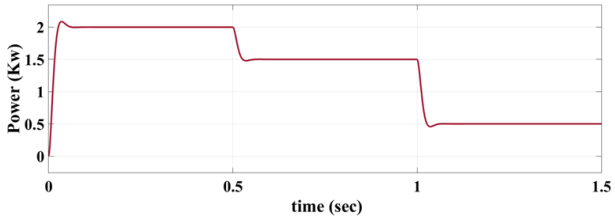

Fig. 14. Simulation results for the single-phase TPC used in a hybrid PVBESS configuration for solar Power at the three ports

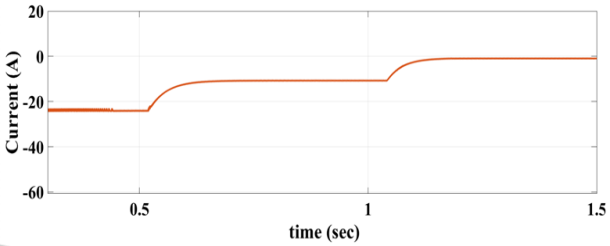

Fig. 15. Simulation results for the single-phase TPC used in a hybrid PVBESS configuration for Current at the battery ports

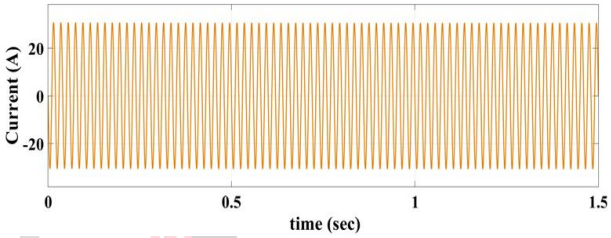

Fig. 16. Simulation results for the single-phase TPC used in a hybrid PVBESS configuration for Grid current

V. CONCLUSION

TPC manages the power of hybrid systems with two dc and one ac port, which lowers topology complexity and increases power density. Each inverter leg functions as a buck boost converter to provide a dc port. Dc and ac ports are separated by inductors. An FLC to lessen V2G data loss and latency is provided in this work. The intelligent controller that is suggested corrects FLC input data based on current node voltage and trend. The grid and MCS conformity of FLC input data is evaluated. stable voltage at the MCS node Data loss and latency due to traditional FLC versus intelligent controller. This novel DC connection eliminates low frequency harmonics, which can hurt batteries or interfere with PV panel MPPT, allowing higher voltage power to be transferred to an ac side. a MIMO non-linear system is modelled to divide power across three ports. In simulations, the FCS-MPC adheres to power configuration references effectively. Simple structures cost less to compute and optimise. Batteries, solar panels, and single-phase and three-phase ac grids can all be used with the converter. The efficiency is on par with typical single-phase grid-connected converters, and research indicates

 DOI : 10.35291/2454-9150.2022.0387

that it can be increased by adjusting the transistor switching frequency, inductor size, and element voltages.

REFERENCES

[1] X. Shen, D. Tan, Z. Shuai, and A. Luo, "Control techniques for bidirectional interlinking converters in hybrid microgrids: Leveraging the advantages of both ac and dc," IEEE Power Electron. Mag., vol. 6, no. 3, pp. 39–47, Sep. 2019.

[2] S. Eftekharnejad, V. Vittal, G. T. Heydt, B. Keel, and J. Loehr, "Impact of increased penetration of photovoltaic generation on power systems," IEEE Trans. Power Syst., vol. 28, no. 2, pp. 893–901, May 2013.

[3] K. Clement-Nyns, E. Haesen, and J. Driesen, "The impact of charging plug-in hybrid electric vehicles on a residential distribution grid," IEEE Trans. Power Syst., vol. 25, no. 1, pp. 371–380, Feb. 2010.

[4] H. Moradisizkoohi, N. Elsayad, and O. A. Mohammed, "A family of three-port three-level converter based on asymmetrical bidirectional halfbridge topology for fuel cell electric vehicle applications," IEEE Trans. Power Electron., vol. 34, no. 12, pp. 11 706–11 724, Dec. 2019.

[5] P. Shamsi and B. Fahimi, "Dynamic behavior of multiport power electronic interface under source/load disturbances," IEEE Trans. Ind. Electron., vol. 60, no. 10, pp. 4500–4511, Oct. 2013.

[6] L. Zhang, X. Hu, Z. Wang, F. Sun, J. Deng, and D. G. Dorrell, "Multiobjective optimal sizing of hybrid energy storage system for electric vehicles," IEEE Trans. Veh. Technol., vol. 67, no. 2, pp. 1027– 1035, Feb. 2018.

[7] H. Mahmood, D. Michaelson, and J. Jiang, "Decentralized power management of a pv/battery hybrid unit in a droop-controlled islanded microgrid," IEEE Trans. Power Electron., vol. 30, no. 12, pp. 7215– 7229, Dec. 2015.

[8] N. Kim and B. Parkhideh, "Pv-battery series inverter architecture: A solar inverter for seamless battery integration with partial-power dc–dc optimizer," IEEE Trans. Energy Convers., vol. 34, no. 1, pp. 478–485, Mar. 2019.

[9] J. Zhang, H. Wu, X. Qin, and Y. Xing, "Pwm plus secondary-side phase-shift controlled soft-switching full-bridge three-port converter for renewable power systems," IEEE Trans. Ind. Electron., vol. 62, no. 11, pp. 7061–7072, Nov. 2015.

[10] K. Wang, R. Zhu, C. Wei, F. Liu, X. Wu, and M. Liserre, "Cascaded multilevel converter topology for large-scale photovoltaic system with balanced operation," IEEE Trans. Ind. Electron., vol. 66, no. 10, pp. 7694–7705, Oct. 2019.

[11] H. Moradisizkoohi, N. Elsayad, M. Shojaie, and O. A. Mohammed, "Pwm plus phase-shift-modulated three-port three-level soft-switching converter using gan switches for photovoltaic applications," IEEE J. Emerg. Sel. Topics Power Electron., vol. 7, no. 2, pp. 636–652, Jun. 2019.

[12] J. Deng, H. Wang, and M. Shang, "A zvs three-port dc/dc converter for high-voltage bus-based photovoltaic systems," IEEE Trans. Power Electron., vol. 34, no. 11, pp. 10 688–10 699, Nov. 2019.

[13] W. Cai, L. Jiang, B. Liu, S. Duan, and C. Zou, "A power decoupling method based on four-switch three-port dc/dc/ac converter in dc microgrid," IEEE Trans. Ind. Appl., vol. 51, no. 1, pp. 336–343, Jan. 2015.

[14] S. Hu, Z. Liang, and X. He, "Ultracapacitor-battery hybrid energy storage system based on the asymmetric bidirectional z -source topology for ev," IEEE Trans. Power Electron., vol. 31, no. 11, pp. 7489–7498, Nov. 2016.

[15] H. Wu, L. Zhu, and F. Yang, "Three-port-converter-based single-phase bidirectional ac–dc converter with reduced power processing stages and improved overall efficiency," IEEE Trans. Power Electron., vol. 33, no. 12, pp. 10 021–10 026, Dec. 2018.

[16] J. Kan, S. Xie, Y. Wu, Y. Tang, Z. Yao, and R. Chen, "Single-stage and boost-voltage grid-connected inverter for fuel-cell generation system," IEEE Transactions on Industrial Electronics, vol. 62, no. 9, pp. 5480– 5490, Sep. 2015.

[17] S. S. Lee and Y. E. Heng, "Improved single-phase split-source inverter with hybrid quasi-sinusoidal and constant pwm," IEEE Transactions on Industrial Electronics, vol. 64, no. 3, pp. 2024–2031, March 2017.

[18] H. Li, Y. Zeng, B. Zhang, T. Q. Zheng, R. Hao, and Z. Yang, "An improved h5 topology with low common-mode current for transformerless pv grid-connected inverter," IEEE Transactions on Power Electronics, vol. 34, no. 2, pp. 1254–1265, Feb 2019.

AUTHORS PROFILE

Dr.J.Srinu Naick received his B.E degree in Electrical & Electronics Engineering from Andhra University Vishakhapatnam AP, India in 2003 and M.Tech with Energetics from NIT Calicut, Calicut, and Kerala, India in 2007. Ph.D with power system from Achiryanagarjuna university in 2019 He is having 18 years of teaching and research experience. He is currently working as Professor in the Department of EEE, Chadalawada Ramanamma Engineering college(Autonomous), JNTUA, Tirupati, Andhra Pradesh, India. His areas of interest are in the Power systems Industrial Drives & FACTS Controllers.

P. Theertha is an Under Graduate student studying IV B.Tech Electrical and Electronics Engineering from Chadalawada Ramanamma Engineering College Tirupati, Chittoor, Andhra Pradesh, India. Her research interests includePower System and Power Electronics.

 DOI : 10.35291/2454-9150.2022.0387